Multichannel Image Restoration in Astronomy

Rafael Molina and Javier Mateos

Departamento de Ciencias de la Computación e Inteligencia Artificial
Universidad de Granada.
18071 Granada. España.

Abstract

Over the last few years quite a lot of research has been devoted to restore astronomical images, but not much work has been reported on the use of multichannel technique to restore such images.

In this work, we apply the Bayesian paradigm to restore multichannel astronomical images. We compare classical methods which are formulated as Bayesian deconvolution techniques and propose a new method based on a multichannel prior distribution that keeps the flux within each channel.

The methods are compared on real multichannel astronomical images.

1 Introduction

The use of image data from multiple frequency bands, multiple time frames, or multiple sensors can be of tremendous value in a number of applications, such as multispectral satellite remote sensing, multisensor robot guidance, multimedium medical diagnosis and obviously astronomical image restoration.

Multichannel image processing differs from single channel image processing because of the redundancy and the complementary feature of information within channels. The processing is much more complicated due to the increased dimension and the need for extracting and exchanging information from and among all channels.

Single channel restoration has been researched extensively during the past couple of decades [6], [7]. Multispectral and multichannel restoration are relatively new areas of image processing research. Decorrelation of the image channels using the Karhunen-Loeve transform [5] has been used prior to restoring the channels individually. Extending linear methods such as Wiener filtering [2]

and least squares restoration [3] has been accomplished successfully, although the accurate estimation of nonstationary cross-channel correlations remains elusive.

Recently multispectral image model for use in Bayesian maximum a posteriori estimation have been proposed (see [9] and [1]). In these works the Gibbs priors contain spatial and spectral cliques functions to impose constrains on the desired restoration or segmentation.

In this paper we present the application of the Bayesian paradigm to the restoration of multichannel images. In section 2 we introduce the paradigm and noise model we use in the papers. In section 4 we examine existing image models to restore multichannel images and propose a new one based on keeping the flux within each channel. A comparative study of the methods used is performed in section 5.

2 Bayesian Paradigm

We will distinguish between f, the 'true' image which would be observed under ideal conditions (i.e. no noise and no distortions produced by blurring and instrumental effects), and g, the observed image. The aim is then to reconstruct f from g. Bayesian methods start with a *prior distribution*, a probability distribution over images f. It is here where we incorporate information on the expected structure within an image. It is also necessary to specify $p(g|f)$, the probability distribution of observed images g if f were the 'true' image. The Bayesian paradigm dictates that inference about the true f should be based on $p(f|g)$ given by

$$p(f|g) = p(g|f)p(f)/p(g) \propto p(g|f)p(f). \tag{1}$$

To show just one restoration it is common (but not obligatory) to choose the mode of $p(f|g)$, that is, to display the image $\hat{f}$ which satisfies

$$\hat{f} \text{ maximizes } p(g|f)p(f). \tag{2}$$

This is known as the MAP (maximum a posteriori) estimate of f.

Let us now examine the degradation and image models.

3 Degradation Model

The following degradation model is considered

$$g = HF + n, \tag{3}$$

where g, f and n represent the observed image, the original image and the noise respectively. For three channels, the same can be applied to k channels, $M \times N$ pixels each, these images are given by

$$g = \begin{pmatrix} g_1 \\ g_2 \\ g_3 \end{pmatrix}, \qquad f = \begin{pmatrix} f_1 \\ f_2 \\ f_3 \end{pmatrix}, \qquad n = \begin{pmatrix} n_1 \\ n_2 \\ n_3 \end{pmatrix}, \tag{4}$$

where each of the $M \times N$ vectors g_i, f_i and n_i results from the lexicographic ordering of the two-dimensional signals in each channel. We will denote by $f_i(u)$ the intensity of the true channel i image at the location of the pixel u on the lattice. The convention applies equally to the observed image g and the noise n.

We shall assume that the $[3(M \times N)] \times [3(M \times N)]$ multichannel degradation matrix H is equal to

$$H = \begin{pmatrix} H_{11} & 0 & 0 \\ 0 & H_{22} & 0 \\ 0 & 0 & H_{33} \end{pmatrix}. \tag{5}$$

This means that in this work we shall assume there is no cross-channel degradation.

So we have

$$p(g|f) \propto \exp\left[-\beta_1 \parallel g_1 - H_{11}f_1 \parallel^2 -\beta_2 \parallel g_2 - H_{22}f_2 \parallel^2 -\beta_3 \parallel g_3 - H_{33}f_3 \parallel^2\right]. \tag{6}$$

u:+3

u:+4 u u:+1

u:+2

Fig. 1. Image sites at each channel.

4 Image Models

Let us first describe the prior model without cross-channel information. Our prior knowledge about the smoothness of the object within each channel makes it possible to model the distribution of f_i for $i = 1, 2, 3$ by a Conditional Autoregressive Model (CAR) (see Ripley [8]). Thus,

$$p(f_i) \propto \exp\left\{-\gamma_i f_i^T (I - \phi N) f_i\right\}, \tag{7}$$

where $N_{uv} = 1$ if cells u and v are spatial neighbors (pixels at distance one), zero otherwise and $\phi = 0.25$. The term $f_i^T(I - \phi N)f_i$ represents in matrix notation the sum of squares of the values $f(u)$ minus ϕ times the sum of $f(u)f(v)$ for neighboring pixels u and v. The parameter α_i measures the smoothness of the 'true' channel i image.

From Eq. 7 we have

$$p(f_i) \propto \exp[-\alpha_i \sum_u [(f(u) - f(u:+1))^2 + (f(u) - f(u:+2))^2]] \tag{8}$$

where $u:+1$, $u:+2$, $u:+3$, $u:+4$ denote the four pixels around pixel u as described in figure 1, $\alpha_i = \phi\gamma_i$ and we assume a 'toroidal edge correction'.

Before describing the models used in the paper, it is very important to note that although in [4] and [3] the methods used are based on Laplacians and so they can be considered as setting constrains on second derivatives we are going to formulate them as methods based on CAR models and so as methods that set constrains on first derivatives.

4.1 Model proposed by Gou, Lee and Teo. Model I.

Although the method proposed in [4] is based on the $3D$ Laplacian and so it could be considered as a Simultaneous Autoregressive Model (SAR), we can easily find its Conditional Autoregressive version. This is given by

$$p(f) \propto$$

$$\exp[-\alpha_{12} \parallel f_1 - f_2 \parallel)^2 - \alpha_{23} \parallel f_2 - f_3 \parallel)^2 - \alpha_{13} \parallel f_1 - f_3 \parallel)^2] \prod_{i=1}^{3} p(f_i), \tag{9}$$

where $p(f_i)$ has been defined in Eq. 8 and $\parallel f_i - f_j \parallel^2 = \sum_u (f_i(u) - f_j(u))^2$ It is very important to note that this model does not normalize each channel and so the square differences involved in the prior may not have much sense.

4.2 Model proposed by Galatsanos, Katsaggelos, Chin and Hillery. Model II.

This method was proposed before the one described in [4] and it takes into account the norm of each channel. The CAR model is given by Eq. 9 but f_i is replaced by $f_i / \parallel f_i \parallel$.

4.3 Alternative model. Model III

One of the problems with models I and II is that they do not keep the flux within each channel. For the degradation model described by Eq. 6 it makes perfect sense to try to keep the flux within each channel. To achieve so we simply replace f_i in Eq. 9 by $f_i / (\sum_u f_i(u))$.

4.4 Model proposed by Schultz and Stevenson. Model IV

The Model proposed in [9] uses 8-neighbors within each channel and instead of using the quadratic edge penalty $\rho(x) = x^2$ uses a Huber-Markov Random Field to model each channel spatially.

Spatial activity measures, the difference between neighbor pixels in each channel, will be used as edge detectors within each channel. Weighted differences of these spatial activity measures are used as the spectral clique functions, with weights estimated to account for edges in one channel that are not present in another (see [9] for details).

5 Test Examples

The models I to IV were tested on the multichannel astronomical images shown in figure 2(a)-(c). They correspond to images of the same object taken

at different wavelength. The range for each image is $[0, 10]$ for figure $2a$, $[0, 24]$ for figure $2b$ and $[0, 62]$ for figure $2c$.

The blurring function, h_{ii} can be approximated by $h_{ii}(r) \propto (1 + r^2/R^2)^{-\delta}$, $i = 1, 2, 3$. We found $\delta \sim 3$ and $R \sim 3.4$ pixels in all the channels.

For models I to IV we used $\alpha_{11} = \alpha_{22} = \alpha_{33} = 0.05$ and $\alpha_{12} = \alpha_{13} = \alpha_{23} = 0.05$. We also used $\beta_1 = \beta_2 = \beta_3 = 0.9$

Figure 3 shows the maximum values of each observed image and the corresponding restorations.

From the experiments we have run we have found that model IV produces too smooth restorations. Model I moves a lot of flux between channels, In our examples increases enormously the flux of image centerh95b and reduces the one of image centerh95r. Models II and III produce similar results but model III seems to produce better restorations maximum values. Model III is the only one that keeps the flux within each channel. Method IV is the only method that does not create objects in channels where they were not present.

Acknowledgments

We would like to thank A. del Olmo and J. Perea, members of the Instituto de Astrofísica de Andalucia, for providing us with the images we have used in this paper.

References

[1] Chang, M.M., Sezan, M.I, A.M. Tekalp and Berg, M.J.,"Bayesian segmentation of multislice brain magnetic resonance imaging using three-dimensional Gibbsian priors", *Optical Engineering*, vol. 35, No. 11, pp 3206–3221, 1996.

[2] Galatsanos, N.P. and Chin, R. T., "Digital Restoration of Multichannel Images", *IEEE Trans. Acoust., Speech, Signal Processing*, vol. 37, No. 3, pp. 415–421, 1989.

[3] Galatsanos, N.P., Katsaggelos, A.K., Chin and R. T., Hillery, A.D., "Least Squares Restoration of Multichannel Images", *IEEE Trans. on Signal Processing*, vol. 39, No. 10, pp. 2222–2236, 1991.

[4] Guo, Y.P., Lee, H.P. and Teo, C.L., "Multichannel Image Restorations Using Iterative Algorithm in Space Domain", *Image and Video Computing*, vol. 14, pp. 389–400, 1996.

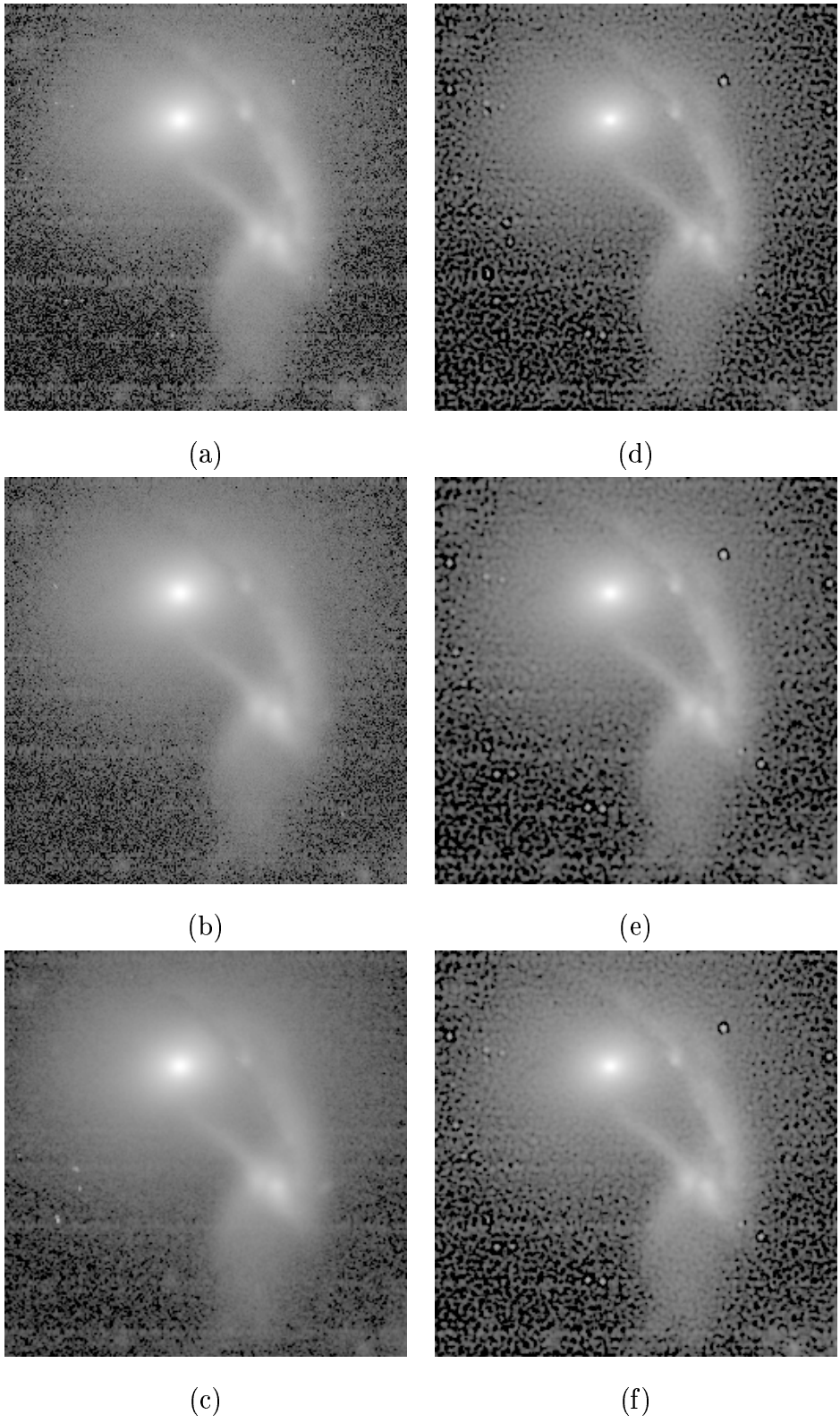

Fig. 2. Observed image at three different wavelength corresponds to (a), (b) and (c). (d) Restoration of (a) using model I. (e) Restoration of (a) using model II and (f) Restoration of (a) using model III.

image	original	Model I	Model II	Model III	Model IV
centerh95b	10	17	13	14	12
centerh95v	24	45	31	39	19
centerh95r	62	78	81	83	75

Fig. 3. Maximum values of the observed and restored images.

[5] Hunt, B.R. and Kübler, O. "Karhunen-Loeve multispectral image restoration, part 1: Theory", *IEEE Trans. Acoust., Speech, Signal Processing*, vol. 32, No. 3, pp. 592–600, 1984.

[6] Katsaggelos, A.K., editor, *Digital Image Restoration*, Springer Series in Information Sciences, vol. 23, Springer-Verlag, 1991.

[7] Nuñez, J. editor, editor, *Image Reconstruction and Restoration in Astronomy*, Special issue of *International Journal of Imaging Systems and Technology* , vol. 6, no 4, 1995.

[8] Ripley, B.D. (1981) "Spatial Statistics", Wiley, New York.

[9] Schultz, R.R., Stevenson, R.L., "Stochastic Modeling and Estimation of Multispectral Image Data", *IEEE Trans. on Image Processing*, vol. **IP**4, No. 8, pp. 1109–1119, 1995.